The Journal of Chemical Physics

Hardness of molecules and bandgap of solids from a generalized gradient approximation exchange energy functional

Cite as: J. Chem. Phys. **157**, 114109 (2022); https://doi.org/10.1063/5.0096678
Submitted: 20 April 2022 • Accepted: 24 August 2022 • Accepted Manuscript Online: 24 August 2022 • Published Online: 20 September 2022

Javier Carmona-Espíndola, Anaid Flores, José L. Gázquez, et al.

View Online Export Citation CrossMark

ARTICLES YOU MAY BE INTERESTED IN

Properties of the density functional response kernels and its implications on chemistry
The Journal of Chemical Physics **157**, 114102 (2022); https://doi.org/10.1063/5.0094653

Scaled σ-functionals for the Kohn–Sham correlation energy with scaling functions from the homogeneous electron gas
The Journal of Chemical Physics **157**, 114105 (2022); https://doi.org/10.1063/5.0101641

Exact two-component Hamiltonians for relativistic quantum chemistry: Two-electron picture-change corrections made simple
The Journal of Chemical Physics **157**, 114106 (2022); https://doi.org/10.1063/5.0095112

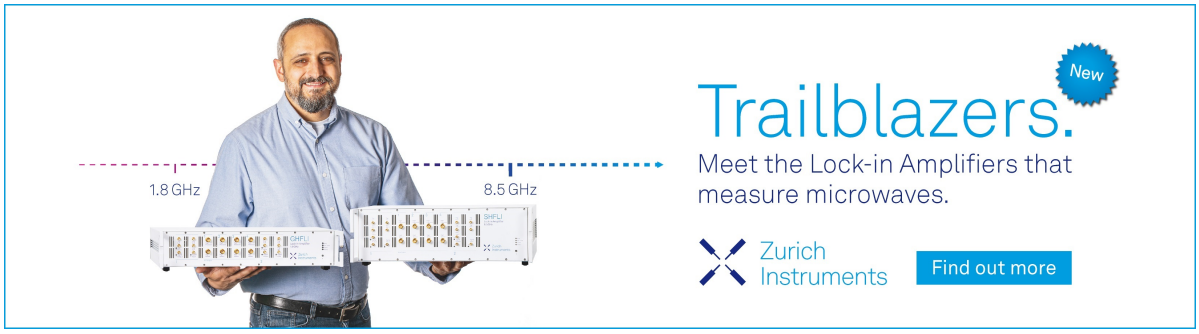

© 2022 Author(s).

AIP Publishing

The Journal of Chemical Physics ARTICLE scitation.org/journal/jcp

Hardness of molecules and bandgap of solids from a generalized gradient approximation exchange energy functional

Cite as: J. Chem. Phys. 157, 114109 (2022); doi: 10.1063/5.0096678
Submitted: 20 April 2022 • Accepted: 24 August 2022 •
Published Online: 20 September 2022 • Corrected: 21 September 2022

View Online Export Citation CrossMark

Javier Carmona-Espíndola,[1,a)] Anaid Flores,[2,b)] José L. Gázquez,[2,c)] Alberto Vela,[3] and S. B. Trickey[4]

AFFILIATIONS

[1] Departamento de Química, CONACYT-Universidad Autónoma Metropolitana-Iztapalapa, Av. San Rafael Atlixco 186, Ciudad de México 09340, Mexico
[2] Departamento de Química, Universidad Autónoma Metropolitana-Iztapalapa, Av. San Rafael Atlixco 186, Ciudad de México 09340, Mexico
[3] Departamento de Química, Centro de Investigación y de Estudios Avanzados, Av. Instituto Politécnico Nacional 2508, Ciudad de México 07360, Mexico
[4] Quantum Theory Project, Department of Physics and Department of Chemistry, University of Florida, P.O. Box 118435, Gainesville, Florida 32611-8435, USA

[a)] **E-mail:** jcarmona_26@yahoo.com.mx
[b)] **E-mail:** anaidgfh@gmail.com
[c)] **Author to whom correspondence should be addressed:** jlgm@xanum.uam.mx

ABSTRACT

The deviations from linearity of the energy as a function of the number of electrons that arise with current approximations to the exchange–correlation (XC) energy functional have important consequences for the frontier eigenvalues of molecules and the corresponding valence-band maxima for solids. In this work, we present an analysis of the exact theory that allows one to infer the effects of such approximations on the highest occupied and lowest unoccupied molecular orbital eigenvalues. Then, we show the importance of the asymptotic behavior of the XC potential in the generalized gradient approximation (GGA) in the case of the NCAPR functional (nearly correct asymptotic potential revised) for determining the shift of the frontier orbital eigenvalues toward the exact values. Thereby we establish a procedure at the GGA level of refinement that allows one to make a single calculation to determine the ionization potential, the electron affinity, and the hardness of molecules (and its solid counterpart, the bandgap) with an accuracy equivalent to that obtained for those properties through energy differences, a procedure that requires three calculations. For solids, the accuracy achieved for the bandgap lies rather close to that which is obtained through hybrid XC energy functionals, but those also demand much greater computational effort than what is required with the simple NCAPR GGA calculation.

Published under an exclusive license by AIP Publishing. https://doi.org/10.1063/5.0096678

I. INTRODUCTION

The Kohn–Sham (KS) realization of density functional theory[1–3] (DFT) has by now come to be recognized as an extraordinarily valuable tool for determining the electronic structure of molecules and solids. However, despite the success in describing charge distributions, total energy differences, and structural properties with KS-DFT and carefully developed approximations to the exchange–correlation (XC) energy functional, there remains a category of shortcomings attributable to a limitation of such approximations. Some of these problems come from the deviations from the exact behavior of the energy as a function of the number of electrons,[4] N. In particular, the accurate determination of the hardness of molecules or its counterpart in solids, the bandgap, remains as one of the important challenges in the KS approach with conventional XC approximations. For a neutral N_0-electron system (N_0 is an integer) in an external potential $v(\mathbf{r})$, the fundamental gap is given by the difference between

Published under an exclusive license by AIP Publishing

the vertical ionization potential (I) and electron affinity (A), that is,

$$E_g = I - A, \tag{1}$$

with

$$I = E(N_0 - 1) - E(N_0) \text{ and } A = E(N_0) - E(N_0 + 1), \tag{2}$$

which implies that the energy gap is calculated through the energies of the $N_0 - 1$, N_0, and $N_0 + 1$ integer electron systems. The hardness of molecules[5] together with the chemical potential,[6] the Fukui function,[7] and the dual descriptor[8,9] are fundamental concepts in the theory of chemical reactivity.[10,11] The bandgap of solids is a very important property for the development of many applications. In principle, at least, determination of E_g through Eq. (1) can be done for solids by calculation of increasing finite size clusters or finite number of primitive unit cells, to extrapolate to infinite size.[12] Thus, with present approximations to the XC functional, $E_{XC}[\rho]$, one can obtain reasonable values of I and A from appropriate energy differences for small size systems, but the results deteriorate as the system size increases. Even on molecular systems, the evaluation of E_g from Eq. (1) requires three calculations, the ground state of the N_0 electron system, and the corresponding $N_0 - 1$ and $N_0 + 1$ electron species at the ground state geometry of the N_0 electron system.

Thus, an alternative approach is to approximate the hardness or bandgap by what is known as the KS gap, E_g^{KS}, namely the difference between the energies of the highest occupied molecular orbital (HOMO) and the lowest unoccupied molecular orbital (LUMO), ε_H and ε_L, respectively, of the N_0 electron system, that is,

$$E_g \approx E_g^{KS} = \varepsilon_L(N_0) - \varepsilon_H(N_0). \tag{3}$$

For this procedure, one only needs to perform the calculation of the reference system ground state. However, as has been well-known for decades, the usual result with common XC functional approximations is a rather severe underestimation of the molecular hardness. Similarly, in solids, there is an improvement in going from the local density approximation (LDA), to the generalized gradient approximation (GGA), and the meta-GGA XC energy functionals, that reaches a rather reasonable accuracy with global and range separated hybrids.[12,13] However, the explicit orbital dependence in E_{XC} of the latter three types of approximate functionals means that the KS scheme is no longer computationally feasible in many cases. Instead, generalized-KS must be used, i.e., the XC potential is nonlocal, which raises both issues of interpretability and computational costs.

Now, the exact behavior of the energy as a function of the number of electrons (at zero temperature) is found to be given[14–19] by lines connecting the integer values of N. This behavior implies that for a neutral reference system with N_0 electrons, $(\partial E/\partial N)^-_{v(\mathbf{r})} = -I$, and $(\partial E/\partial N)^+_{v(\mathbf{r})} = -A$, where the minus and plus superscript signs are used to indicate that the derivatives are evaluated from the electron deficient and the electron abundant sides of N_0, respectively. Thus, one can see that the hardness or bandgap may also be expressed as[13,20–22]

$$E_g = \left(\frac{\partial E}{\partial N}\right)^+_{v(\mathbf{r})} - \left(\frac{\partial E}{\partial N}\right)^-_{v(\mathbf{r})} = I - A. \tag{4}$$

Although this expression holds for the exact Kohn–Sham energy and derivatives evaluated at $N = N_0$, when those derivatives are evaluated with an approximate XC functional, the results may differ (and typically do differ substantially) from those exact values. The deviations from the exact values have been identified as fractional charge errors,[20,21] which may be of two types. When the deviation from strict linearity is a convex curve, it is identified as a delocalization error. In the case of a concave curve, the deviation is identified as a localization error.

For molecules, it has been found that LDA, GGA, and meta-GGA XC functionals yield a rather large convex curve for fractional charges[23] that leads to substantial errors in the hardness when determined through Eq. (4). On the other hand, since global hybrids and range-separated hybrids compensate for the spurious convexity partially through the concave component introduced by the fraction of single-determinant exchange,[23] those more complicated XC functionals provide, generally, a better description of the values of E_g determined from Eq. (4). Additional improvement to practically reach the linear behavior is obtained through long-range corrected functionals[24] like MCY3,[25] but the results deteriorate as the size of the system increases. For solids, it has been found through the analysis of the fractional charge error that although the piecewise linearity of the energy is practically recovered in very large and bulk systems,[21,26] for any XC functional, it is quantitatively different from the exact linearity because of the delocalization error that characterizes convex functionals.[21] Notice also that there is a crucial difference between Eq. (1) and the analysis in Ref. 26. Eq. (1), applied to any finite system, involves one neutral system and two charged ones. The analysis by which Ref. 26 arrives at the conclusion of piecewise linearity for a solid with any XC functional is for three *neutral* systems, differing in electron population per cell by one. That neutrality is required for convergence of the relevant lattice sums. Thus, the analysis of Ref. 26 is not equivalent to the infinite system limit of finite clusters mentioned in Ref. 12. This ambiguity about the infinite system limit is another motivation for seeking a systematic way to calculate and correct KS eigenvalues to give $E_g^{KS} \approx E_g$ to acceptable accuracy in both molecules or solids.

To improve the values of the left and right derivatives of Eq. (4) of approximate XC energy functionals, one can make use of corrections to impose the linear behavior of the energy.[13,27] Alternatively, one can take into account the effects of the discontinuity implied in the functionals as N crosses an integer value. Pursuing this latter approach, Görling[28] has shown that the derivative discontinuity (DD) is directly measurable by the non-zero constant needed to make the XC potential vanish asymptotically. In this direction, recently we proposed a GGA XC energy functional, NCAP (nearly correct asymptotic potential)[29] whose functional derivative tends asymptotically to a constant that depends on the HOMO eigenvalue. Through that relationship, one[30] can identify the discontinuity contained in Eq. (4). That work did not exploit fully the opportunity provided by a good estimate of the discontinuity contribution. Thus, the objective of the present work is to make a mild revision of NCAP, which we will call nearly correct asymptotic potential revised (NCAPR), to determine the hardness of molecules and bandgaps of

Published under an exclusive license by AIP Publishing

solids through just one reasonably accurate, computationally very simple, and inexpensive GGA calculation of the ground state.

II. THEORETICAL DEVELOPMENT

The discontinuity contained in Eq. (4) implies that the XC potential $v_{XC}(\mathbf{r})$, which is given by the functional derivative of the XC energy, $E_{XC}[\rho]$, with respect to the electron density, $\rho(\mathbf{r})$, also presents a discontinuity as the number of electrons N crosses an integer value,[31–34]

$$\Delta_{XC} = v^{+}_{XC}(\mathbf{r}) - v^{-}_{XC}(\mathbf{r}), \tag{5}$$

where Δ_{XC} is the magnitude of the derivative discontinuity (DD), which is assumed to be constant.[35] For the exact Kohn–Sham theory, the ionization potential theorem indicates that[34]

$$\varepsilon^{-}_{H} = -I \tag{6}$$

and

$$\varepsilon^{+}_{L} = -A, \tag{7}$$

where ε^{-}_{H} is the HOMO eigenvalue of the N electron system determined with $v^{-}_{XC}(\mathbf{r})$, and ε^{+}_{L} is the LUMO eigenvalue determined with $v^{+}_{XC}(\mathbf{r})$. Combining these expressions with Eq. (1), one obtains

$$E_g = I - A = \varepsilon^{+}_{L} - \varepsilon^{-}_{H}. \tag{8}$$

On the other hand, since Δ_{XC} is constant, one finds via Eq. (5) that

$$\Delta_{XC} = \varepsilon^{+}_{L} - \varepsilon^{-}_{L}, \tag{9}$$

where ε^{-}_{L} is the eigenvalue of the LUMO determined with $v^{-}_{XC}(\mathbf{r})$. Therefore, substituting this last expression in Eq. (8) and using Eq. (3) gives

$$E_g = \varepsilon^{-}_{L} - \varepsilon^{-}_{H} + \Delta_{XC} = E^{KS}_{g} + \Delta_{XC}. \tag{10}$$

This confirms that, indeed, the KS gap obtained through XC functionals that do not incorporate the derivative discontinuity of the corresponding XC potential underestimate the true gap.

Now, it has been shown[20] that the derivatives in Eq. (4) may be expressed in terms of the eigenvalues of the frontier orbitals (valence band maxima, conduction band minima in solids), that is,

$$\left(\frac{\partial E}{\partial N}\right)^{-}_{v(\mathbf{r})} = \left(\frac{\partial E}{\partial n_H}\right)^{-}_{v_S(\mathbf{r})} = \varepsilon^{-}_{H} \tag{11}$$

and

$$\left(\frac{\partial E}{\partial N}\right)^{+}_{v(\mathbf{r})} = \left(\frac{\partial E}{\partial n_L}\right)^{+}_{v_S(\mathbf{r})} = \varepsilon^{+}_{L}, \tag{12}$$

where $v_S(\mathbf{r})$ is the total Kohn–Sham potential given by the sum of the external, the Columbic and the XC potentials, n_H is the HOMO occupation, and n_L is the LUMO occupation.

Thus, it is important to note that either the analysis based on the derivative discontinuity of the XC potential or the one based on the derivatives of the energy with respect to the number of electrons leads to the same result. However, the latter approach has the advantage of showing that the error in the calculation of the bandgap with approximate XC potentials comes from the fractional charge error associated with the evaluation of the derivative of the energy with respect to the number of electrons in the limit when $N \to N_0$. As noted, it has been identified as a delocalization error for XC functionals that have a convex $E(N)$ curve in the case of finite systems. The error persists in solids despite their linear behavior because of having incorrect slopes.

Now, the DD may be decomposed[30] through the following analysis. First, rewrite Eqs. (6) and (7) in the form

$$\varepsilon^{-}_{H} = -I = \varepsilon^{-}_{H} - (\varepsilon^{-}_{H} + I) \text{ and } \varepsilon^{+}_{L} = -A = \varepsilon^{-}_{L} - (\varepsilon^{-}_{L} + A), \tag{13}$$

where ε^{-}_{H} and ε^{-}_{L} are obtained through a Kohn–Sham calculation of the reference system with the exact or with an approximate exchange–correlation potential. The terms in parenthesis may be interpreted as the shifts one has to perform on the eigenvalues to obtain the exact I and A. Thus, one can define these shifts as

$$\Delta^{-}_{XC} = -(\varepsilon^{-}_{H} + I) \text{ and } \Delta^{+}_{XC} = -(\varepsilon^{-}_{L} + A), \tag{14}$$

and from these two expressions and Eq. (10), one can see that

$$\Delta_{XC} = \Delta^{+}_{XC} - \Delta^{-}_{XC}. \tag{15}$$

For the exact Kohn–Sham XC functional, $\Delta^{-}_{XC} = 0$ because of Eq. (6), and $\Delta^{+}_{XC} = \Delta_{XC}$ because of Eqs. (7) and (9). However, for an approximate XC energy functional, e.g., a GGA, then $\Delta^{-}_{XC} \neq 0$, $\Delta^{+}_{XC} \neq 0$, and the corresponding non-zero Δ_{XC} is given by Eq. (15).

A GGA exchange energy functional typically is expressed in terms of an enhancement factor $F_X(s)$ where the reduced density gradient $s(\mathbf{r}) = |\nabla\rho(\mathbf{r})|/2k_F\rho(\mathbf{r})$, with $k_F = (3\pi^2\rho(\mathbf{r}))^{1/3}$, that is,

$$E^{GGA}_{X}[\rho] = \int \rho(\mathbf{r})\, \varepsilon^{LDA}_{X}(\rho(\mathbf{r}))\, F_X(s)\, d\mathbf{r}, \tag{16}$$

where $\varepsilon^{LDA}_{X}(\rho(\mathbf{r})) = A_X(\rho(\mathbf{r}))^{1/3}$ is the local density approximation per particle and $A_X = -3(3\pi^2)^{1/3}/4\pi$. Our recent[29] NCAP X functional has the enhancement factor

$$F^{NCAP}_{X}(s) = 1 + \mu \tanh(s) \sinh^{-1}(s) \frac{1 + \alpha\left((1-\varsigma)\, s \ln(1+s) + \varsigma\, s\right)}{1 + \beta \tanh(s) \sinh^{-1}(s)}. \tag{17}$$

Its parameters μ, α, β, and ς are determined through the fulfillment of constraints associated with the physically important region that lies in the interval $0 \le s \le 3$ and through the imposition of constraints corresponding to the limit when $s \to \infty$. In that limit, the enhancement factor goes to

$$F^{NCAP}_{X}(s) \xrightarrow[s\to\infty]{} \frac{4\pi}{3}\left((1-\varsigma)\, s \ln(1+s) + \varsigma\, s\right), \tag{18}$$

which corresponds to a linear combination of the term $s\ln(1+s)$ and the term s. The former type leads to an X potential

Published under an exclusive license by AIP Publishing

contribution that goes asymptotically to a constant plus a term that decays as r^{-1}, while the second type leads to an X potential that decays as r^{-1}. A crucial point is that NCAP includes both types; hence, its intrinsic X potential goes asymptotically to a non-zero constant.

Now, the asymptotic behavior of the electronic density is given by[36–38]

$$\rho(\mathbf{r}) \xrightarrow[r\to\infty]{} \rho_0\, e^{-\lambda r} \quad \lambda = 2\sqrt{-2\varepsilon_H^-}. \tag{19}$$

It is important to mention that this expression is valid only when the exchange–correlation potential goes asymptotically to zero. Thus ε_H^- must corresponds to a shifted $v_X^-(\mathbf{r})$ satisfying this condition. Now, replacing this behavior in the expression that results from the functional derivative of the exchange energy with respect to the electron density, $v_X^{NCAP}(\mathbf{r}) = \delta E_X^{NCAP}[\rho(\mathbf{r})]/\delta\rho(\mathbf{r})$ means that the variationally determined X potential, therefore, behaves asymptotically as

$$v_X^{NCAP}(\mathbf{r}) \xrightarrow[r\to\infty]{} -A_X\, Q_X\sqrt{-\varepsilon_H^-} - c/r, \tag{20}$$

where A_X is defined in Eq. (16), $Q_X = (\sqrt{2}/3(3\pi^2)^{1/3})\gamma$ with $\gamma = 4\pi(1-\varsigma)/3$ and c is a constant whose value[29] is expected to be around 0.3, instead of 1. For this reason, the exchange energy functional was named NCAP (nearly correct asymptotic potential). Because A_X is negative, the constant in Eq. (20) is positive [as corroborated by numerical values of $v_X^{NCAP}(\mathbf{r})$] and one can define the quantity

$$v_X^{DD} = A_X\, Q_X\sqrt{-\varepsilon_H^-}. \tag{21}$$

Thus, since the fulfillment of Eq. (19) and the ionization potential theorem require that the exchange potential must be realigned to zero asymptotically, one needs to add the constant in Eq. (21) to the NCAP exchange potential, that is,

$$v_X^-(\mathbf{r}) = v_X^{NCAP}(\mathbf{r}) + v_X^{DD}, \tag{22}$$

so that

$$\varepsilon_H^- = \varepsilon_H^{NCAP} + v_X^{DD}, \tag{23}$$

where ε_H^{NCAP} is the eigenvalue directly obtained in the SCF Kohn–Sham calculation with the unshifted NCAP exchange potential associated with the highest occupied molecular orbital. It must be shifted according to Eq. (23), to obtain the value ε_H^-, which is the one that satisfies the ionization potential theorem, which one expects to be closer to the exact $-I$.

Clearly, it is more convenient to express the constant given in Eq. (21) in terms of ε_H^{NCAP} instead of ε_H^-, since it is the eigenvalue obtained directly in the SCF Kohn–Sham calculation. Therefore, substituting ε_H^- from Eq. (21) in Eq. (23) leads to a quadratic equation in v_X^{DD}, whose solutions are[30,39]

$$v_X^{DD\mp} = -\frac{1}{2}A_X^2\, Q_X^2\left(1 \pm \sqrt{1 - 4\frac{\varepsilon_H^{NCAP}}{A_X^2\, Q_X^2}}\right). \tag{24}$$

Consequently, given that Δ_{XC}^- should be a negative quantity and that v_X^{DD-} satisfies this condition, we make the identification $v_X^{DD-} \approx \Delta_{XC}^-$ so that

$$\varepsilon_H^- = -I = \varepsilon_H^{NCAP} + v_X^{DD-}, \tag{25}$$

and similarly, since Δ_{XC}^+ should be a positive quantity, a condition satisfied by v_X^{DD+}, we also make the identification $v_X^{DD+} \approx \Delta_{XC}^+$, which implies that

$$\varepsilon_L^+ = -A = \varepsilon_L^{NCAP} + v_X^{DD-}. \tag{26}$$

Using that $\varepsilon_L^- = \varepsilon_L^{NCAP} + v_X^{DD-}$, together with Eq. (26) in Eq. (9), leads to the relation

$$\Delta_{XC} = v_X^{DD+} - v_X^{DD-}. \tag{27}$$

This argument establishes that the difference between the two roots of Eq. (24) provides an estimate of the DD magnitude. Verification of the validity of the two identifications is provided by the quality of the results presented in Sec. III, together with the fact that the analysis that led to Eqs. (14) and (15) indicates that for an approximate exchange–correlation energy functional the shift for ε_H^{NCAP} required to get closer to $-I$ is different from the shift for ε_L^{NCAP} required to get closer to $-A$, and the numerical evidence shows that the shift for ε_H^{NCAP} must be negative, while the shift for ε_L^{NCAP} must be positive.

In the original NCAP,[29] we fixed $\mu = 0.219\,515$, which corresponds to the PBE value.[40] We used $\beta = 0.018\,086$ that comes from the exact cancellation via the X term of the Coulomb self-repulsion for the exact hydrogen atom density. In NCAP, we also fixed $\varsigma = 0.304\,121$ by imposing the specific value of v_X^{DD-} in Eq. (25) that gives the exact ionization potential of the hydrogen atom. The parameter $\alpha = 4\pi\beta/3\,\mu = 0.345\,112$ was fixed by the asymptotic conditions. We found that this X energy functional, when combined with the Perdew-86 correlation energy functional,[41] provides a description of thermodynamic, kinetic, and structural properties of molecules close to the accuracy obtained through meta-GGA and global hybrid XC functionals. Moreover, because of the asymptotic behavior imposed, it also leads to a rather good description of response properties and excitation energies. It was also found that although the eigenvalues obtained from NCAP by itself are similar to those obtained from any other GGA, the corrections introduced in Eqs. (25) and (26) provide a better description of the ionization potential[29] and the electron affinity[30] of molecules. However, in general, NCAP values of those quantities tend to be overestimated. This overestimation can be traced, in part, to the value $\varsigma = 0.304\,121$. As can be seen in Eq. (18), this value gives more weight to the term $s\ln(1+s)$ than the term s. However, one may adopt a different viewpoint. Although both terms lead to a $-\text{constant}/r$ behavior, they do have a different dependence on the reduced density gradient s. In the absence of any rigorous result that compels a value of ς, it is a matter of design choice. The choice in NCAP was an "appropriate norm."

Published under an exclusive license by AIP Publishing

However, that turns out to bias the functional unhelpfully. An alternative design choice is the plausible criterion to give the same weight to both terms, by setting the value to $\varsigma = 1/2$. The parameter β can be determined by recalling the exact DFT result that, for the hydrogen atom, the exchange energy cancels the classical Coulomb repulsion. That gives $\beta = 0.017\,983$. All the other parameter values are unchanged from NCAP. We designate this reparameterized version as NCAPR. In the supplementary material, we show that the effect of this parameter modification upon all the previously tested thermochemical properties is very small so that the performance of NCAPR is essentially the same as for NCAP on standard molecular datasets in the calculation of energy differences and electronic densities. However, there are important differences in the shifts that need to be applied in Eqs. (25) and (26) to determine through them the hardness of molecules and the bandgap of solids so that the quality of the results presented in Sec. III also provides support for $\varsigma = 1/2$.

It is important to note that with the value of $\varsigma = 1/2$, the shifted eigenvalue of the ground state of the hydrogen atom is −0.42 instead of −0.5, and the asymptotic potential is given by

$$v_X^{NCAP}([\rho];\mathbf{r}) \xrightarrow[r\to\infty]{} 0.153\,01 - 0.467\,84/r. \tag{28}$$

Since it is estimated that the values for any finite system in this limit will be close to those of the hydrogen atom, one can see that this reparameterized version will lead to a nearly correct asymptotic potential (NCAP) since it decays as $-c/r$, with a value of c around 0.5.

It is worth reiterating a point that may have been obscured through the detail of analysis, namely, that by use of Eqs. (25) and (26), one may calculate the molecular hardness or the solid bandgap with just one NCAPR calculation of the ground state of the neutral reference system.

III. RESULTS AND DISCUSSION

To establish the comparative performance of NCAPR, we have considered several XC energy functionals, PBE[40] at the GGA level of refinement, SCAN[42] that belongs to the meta-GGA level, the global hybrid PBE0,[43,44] and the range separated hybrid HSE06,[45,46] together with a test set of 83 molecules with positive (45) and negative (38) electron affinities, and a test set of 70 solids for which the band gaps range from small to large values.

For molecules, the test set contains 36 species with positive A values taken from Ref. 13 whose geometries were optimized with B3LYP[47–49]/6-31G*[50,51] and 9 from Ref. 52 with geometries determined with B3LYP/6-31G(2df,p)[53] calculations. The group of 38 species with negative A values is the same as the one used in Refs. 27 and 30, with the geometries obtained with B3LYP/6-311+G**.[54] Those geometries were used to determine the energies of the reference system and its corresponding cation and anion, with the aug-cc-pVTZ basis set.[55,56] The calculations were done with a modified version of NWChem 6.5.[57]

In Table I, we present the mean absolute deviations (MAD) in the 83 molecules test set for the ionization potential I, the electron affinity A, and the hardness obtained from energy differences (that require three calculations, the reference system and its corresponding cation and anion). We also present in Table I the values obtained for those three quantities through the frontier eigenvalues

TABLE I. Mean absolute deviations from the experimental values of the ionization potential (I), the electron affinity (A) and the hardness (E_g) for several XC energy functionals for a test set of 83 molecules in eV.

Property	PBE96	NCAPR	SCAN	PBE0	HSE06	NCAPR[a]
Energy differences (three calculations)						
I	0.39	0.40	0.38	0.32	0.33	
A	0.49	0.54	0.55	0.58	0.55	
E_g	0.73	0.81	0.79	0.79	0.74	
Frontier eigenvalues (one calculation)						
I	3.65	3.62	3.37	2.34	2.73	0.58
A	2.86	2.83	2.52	1.79	2.16	0.64
E_g	6.51	6.45	5.89	4.12	4.90	0.91

[a]With the frontier eigenvalues shifted according to Eqs. (25) and (26).

ε_H and ε_L of the N_0 electron system calculated with the various XC approximations, and finally, we also report the results obtained for NCAPR incorporating the frontier eigenvalue shifts indicated in Eqs. (25) and (26), with a single ordinary ground state calculation for each system. One can see that, as anticipated in Eq. (10), the unmodified frontier eigenvalue differences that corresponds to E_g^{KS} give a very poor description of I, A, and hardness for all the functionals considered. It is noteworthy that even the hybrids perform only slightly better than the rest. In marked contrast, the NCAPR shifted values for I, A, and the hardness lie very close to the values calculated by total energy differences. In the supplementary material, we report the results for each molecule of the test set, together with the experimental values of I and A used to determine the MAD.

For solids, corresponding calculations were performed using a modified version of the Vienna *ab initio* simulation package (VASP, version 5.4.4),[58–61] within the projector augmented wave formalism (PAW).[62] We used the pseudopotentials with the version 3.3.5 of VASP (this is common practice, as meta-GGA PAW datasets are not available in VASP). The geometries were extracted from the experimental information in the Materials Project database. We calculated all bandgaps as the difference of the conduction band minimum and valence band maximum, with the NCAP eigenvalue of the HOMO referred to the Fermi level reported in VASP. We used grids with densities ranging from 500 to 4000 k-points per atom and 600 eV cut-off energy. The KS bandgap values for SCAN, PBE0, and HSE06 XC functionals were taken from the supplementary material of Ref. 63.

The test set for solids consists of 70 species divided in four groups determined by species and bandgap magnitude.[64] There are 15 semiconductors with small E_g, between 0 and 2.0 eV, 29 semiconductors with intermediate E_g, between 2.0 and 6.5 eV, 9 ionic compounds with wide E_g, between 7.0 and 14.2 eV, 4 rare-gas crystals insulators with large E_g, between 9.2 and 21.5 eV, and 9 layered materials with E_g between 1.0 and 3.0 eV.

In Table II, we report the MAD for each of the groups and the overall performance. Individual E_g values for each one of the solids in the test set are presented in the supplementary material. One can see that, at the GGA (PBE and the unshifted NCAPR eigenvalues) and meta-GGA levels of refinement, the overall tendency is the well-known bandgap underestimation. Because of it, for the systems with small bandgaps, namely the group of semiconductors with

Published under an exclusive license by AIP Publishing

TABLE II. Mean absolute deviations from the experimental values of the bandgap (E_g) for several XC energy functionals for each group of solids in eV. The groups have increasing band gaps as one moves down and the number in parenthesis indicates the number of solids in each group.

Group	PBE96	NCAPR	SCAN	PBE0	HSE06	NCAPR[a]
Frontier eigenvalues – Conduction and valence bands (one calculation)						
Small (15)	0.65	0.55	0.50	0.61	0.12	1.02
Layered (11)	0.75	0.70	0.48	0.70	0.23	1.14
Intermediate (29)	1.61	1.56	1.24	0.38	0.49	0.50
Ionic (11)	3.47	3.47	2.75	1.34	1.91	1.81
Insulators (4)	5.67	5.27	4.82	3.34	3.95	3.67
Total (70)	1.79	1.72	1.40	0.80	0.79	1.10

[a]With the frontier eigenvalues shifted according to Eqs. (25) and (26).

this characteristic and the layered materials, one obtains relatively low MAD values. However, they increase significantly as the experimental bandgap grows. In the case of the global hybrid PBE0, one obtains a poor description of the layered compounds and the small bandgap semiconductors in comparison with HSE06, which leads to a very good description of these systems; however, the results are similar for all the other groups. Finally, applying the shift indicated by Eqs. (25) and (26), one can see that in the case of the layered systems and the small bandgap semiconductors, the NCAPR-based procedure tends to overestimate the bandgap values. However, it provides a very good description of the intermediate bandgap insulators, and a reasonable one of the ionic species, with values that lie between the PBE0 and HSE06 values. The MAD value for the insulators also lies in between the hybrid functionals. From the perspective of overall performance, we note that the direct eigenvalues from GGA XC functionals lead to the worst description that is improved slightly with the meta-GGA SCAN (which involves generalized KS calculations). The best description corresponds to the hybrids. However, the shifted NCAPR eigenvalues get very close to those obtained from the hybrids. This is an important result because solid system calculations with a fraction of single-determinant exchange are computationally much more demanding than those done with GGA XC energy functionals.

A comparison with other test sets[13,65,66] is presented in the supplementary material, where one can see similar results to the ones obtained in Table II.

Additionally, since all the calculations for solids were done at the experimental geometry, we did a geometry optimization with NCAPR in a subset of ten solids, which cover a wide range of bandgap values, and found that the difference between the calculation with the experimental geometries and the one with the NCAPR geometries in the mean absolute error is rather small, around 0.25 eV, as can be seen in the supplementary material.

IV. CONCLUDING REMARKS

The physical insights provided by the analysis of the behavior of the energy as a function of the number of electrons, specifically the characterization of the deviations from linearity with electron number that arise with current XC functional approximations, allow one to get a better understanding of the impact that those deviations have on the frontier eigenvalues of molecules or solids, especially when those eigenvalues are used to determine the hardness and the bandgap.[20,21] By exploitation of this viewpoint, a natural procedure to correct the situation has been proposed that uses global scaling corrections on approximate XC energy functionals to impose the correct linear behavior.[13]

On the other hand, the perspective provided by the DD of the XC potential and its consequent effects on the frontier eigenvalues and in the calculation of E_g indicates that one can also proceed through the incorporation of these effects in carefully designed, constraint-based approximate XC energy functionals. This latter approach is the one we have adopted in this work. We have presented a very modest revision of our NCAP GGA XC functional that leads to an XC potential that in the asymptotic limit goes to a non-zero constant. Since the DFT ionization potential theorem requires that the potential should go to zero asymptotically, that non-zero constant implies a potential shift. As we have shown, it is directly related to the DD. In fact, we have demonstrated that, in an approximate GGA, one needs to apply different shifts to the HOMO and LUMO eigenvalue and that the sum of these two shifts leads to the magnitude of the DD. The two shifts are determined through the two roots of the quadratic equation that results when the asymptotic constant of the X potential is expressed in terms of the HOMO eigenvalue of the NCAPR calculation.

Thus, we have established a procedure at the GGA level of refinement that allows one to utilize a single calculation to obtain the ionization potential, the electron affinity and the hardness of molecules, and the bandgap of solids. The accuracy reached for molecules is equivalent to that obtained for these properties through energy differences, which require three calculations. For solids, the accuracy achieved for the bandgap lies rather close to the accuracy obtained through hybrid XC energy functionals, which demand great computational effort due to the presence of a fraction of single-determinant exchange. It is important to mention that the accuracy obtained in the present approach for bandgaps is also equivalent, in general, to the one obtained with a meta-GGA that introduces an approximate estimate of the DD through the generalized Kohn–Sham formalism.[64,66]

The overall performance of NCAPR shows that indeed one can obtain a rather good description of the hardness of molecules and the bandgap of solids at the GGA level if one corrects the delocalization error in the frontier eigenvalues by incorporating the derivative discontinuity effects.

Published under an exclusive license by AIP Publishing

SUPPLEMENTARY MATERIAL

See the supplementary material for the values of all the individual systems that conform the test sets for all the functionals and quantities reported in Tables I and II. Additionally, one can find the comparison between NCAP and NCAPR for all the test sets used to validate the original NCAP[29] and the comparison in solids with other test sets.

ACKNOWLEDGMENTS

We are grateful to Xiao Zheng and Weitao Yang for providing us a great part of the optimized geometries of the test set used for molecules. We thank the Laboratorio Nacional de Cómputo de Alto Desempeño for the use of their facilities through the Laboratorio de Supercómputo y Visualización of Universidad Autónoma Metropolitana-Iztapalapa. J.C.-E., J.L.G., and A.V. were supported, in part, by Conacyt through Sinergia (Grant No. 1561802). S.B.T. was supported by U.S. NSF (Grant No. DMR-1912618).

AUTHOR DECLARATIONS

Conflict of Interest

The authors have no conflicts to disclose.

Author Contributions

Javier Carmona-Espíndola: Conceptualization (lead); Formal analysis (lead); Investigation (lead); Methodology (lead); Software (lead); Validation (lead); Writing – original draft (equal); Writing – review & editing (equal). **Anaid Flores**: Conceptualization (equal); Formal analysis (equal); Investigation (equal); Methodology (equal); Validation (equal); Writing – original draft (supporting); Writing – review & editing (supporting). **José L. Gázquez**: Conceptualization (lead); Formal analysis (lead); Investigation (lead); Methodology (lead); Validation (lead); Writing – original draft (lead); Writing – review & editing (lead). **Alberto Vela**: Conceptualization (supporting); Formal analysis (supporting); Writing – original draft (supporting); Writing – review & editing (supporting). **S. B. Trickey**: Conceptualization (supporting); Formal analysis (supporting); Writing – original draft (supporting); Writing – review & editing (supporting).

DATA AVAILABILITY

The data that support the findings of this study are available within the article and its supplementary material.

REFERENCES

[1] P. Hohenberg and W. Kohn, "Inhomogeneous electron gas," Phys. Rev. B **136**, B864–B871 (1964).
[2] W. Kohn and L. J. Sham, "Self-consistent equations including exchange and correlation effects," Phys. Rev. **140**, A1133–A1138 (1965).
[3] R. G. Parr and W. Yang, *Density Functional Theory of Atoms and Molecules* (Oxford University Press, New York, 1989).
[4] A. J. Cohen, P. Mori-Sánchez, and W. Yang, "Challenges for density functional theory," Chem. Rev. **112**, 289–320 (2012).
[5] R. G. Parr and R. G. Pearson, "Absolute hardness: Companion parameter to absolute electronegativity," J. Am. Chem. Soc. **105**, 7512–7516 (1983).
[6] R. G. Parr, R. A. Donnelly, M. Levy, and W. E. Palke, "Electronegativity: Density functional viewpoint," J. Chem. Phys. **68**, 3801–3807 (1978).
[7] R. G. Parr and W. Yang, "Density functional approach to the frontier-electron theory of chemical reactivity," J. Am. Chem. Soc. **106**, 4049–4050 (1984).
[8] C. Morell, A. Grand, and A. Toro-Labbé, "New dual descriptor for chemical reactivity," J. Phys. Chem. A **109**, 205–212 (2005).
[9] C. Morell, A. Grand, and A. Toro-Labbé, "Theoretical support for using the $\Delta f(r)$ descriptor," Chem. Phys. Lett. **425**, 342–346 (2006).
[10] *Chemical Reactivity Theory: A Density Functional View*, edited by P. K. Chattaraj (CRC Press, Boca Raton, 2009).
[11] P. Geerlings, E. Chamorro, P. K. Chattaraj, F. De Proft, J. L. Gázquez, S. Liu, C. Morell, A. Toro-Labbé, A. Vela, and P. Ayers, "Conceptual density functional theory: Status, prospects, issues," Theor. Chem. Acc. **139**, 36 (2020).
[12] J. P. Perdew, W. Yang, K. Burke, Z. Yang, E. K. U. Gross, M. Scheffler, G. E. Scuseria, T. M. Henderson, I. Y. Zhang, A. Ruzsinszky, H. Peng, J. Sun, E. Trushin, and A. Görling, "Understanding band gaps of solids in generalized Kohn-Sham theory," Proc. Natl. Acad. Sci. U. S. A. **114**, 2801–2806 (2017).
[13] X. Zheng, A. J. Cohen, P. Mori-Sánchez, X. Hu, and W. Yang, "Improving band gap prediction in density functional theory from molecules to solids," Phys. Rev. Lett. **107**, 026403 (2011).
[14] J. P. Perdew, R. G. Parr, M. Levy, and J. L. Balduz, Jr., "Density-functional theory for fractional particle number: Derivative discontinuities of the energy," Phys. Rev. Lett. **49**, 1691–1694 (1982).
[15] W. Yang, Y. Zhang, and P. W. Ayers, "Degenerate ground states and a fractional number of electrons in density and reduced density matrix functional theory," Phys. Rev. Lett. **84**, 5172–5175 (2000).
[16] P. W. Ayers, "The dependence on and continuity of the energy and other molecular properties with respect to the number of electrons," J. Math. Chem. **43**, 285–303 (2008).
[17] J. L. Gázquez, in *Chemical Reactivity Theory: A Density Functional View*, edited by P. K. Chattaraj (CRC Press, Boca Raton, 2009), pp. 7–22.
[18] M. Franco-Pérez, J. L. Gázquez, P. W. Ayers, and A. Vela, "Revisiting the definition of the electronic chemical potential, chemical hardness, and softness at finite temperatures," J. Chem. Phys. **143**, 154103 (2015).
[19] J. L. Gázquez, M. Franco-Pérez, P. W. Ayers, and A. Vela, in *Chemical Reactivity in Confined Systems: Theory, Modelling and Applications*, edited by P. K. Chattaraj and D. Chakraborty (Wiley, NJ, 2021), pp. 191–211.
[20] A. J. Cohen, P. Mori-Sánchez, and W. Yang, "Fractional charge perspective on the band gap in density-functional theory," Phys. Rev. B **77**, 115123 (2008).
[21] P. Mori-Sánchez, A. J. Cohen, and W. Yang, "Localization and delocalization errors in density functional theory and implications for band-gap prediction," Phys. Rev. Lett. **100**, 146401 (2008).
[22] W. Yang, A. J. Cohen, and P. Mori-Sánchez, "Derivative discontinuity, bandgap and lowest unoccupied molecular orbital in density functional theory," J. Chem. Phys. **136**, 204111 (2012).
[23] P. Mori-Sánchez, A. J. Cohen, and W. Yang, "Many-electron self-interaction error in approximate density functionals," J. Chem. Phys. **125**, 201102 (2006).
[24] T. Tsuneda, J.-W. Song, S. Suzuki, and K. Hirao, "On Koopmans' theorem in density functional theory," J. Chem. Phys. **133**, 174101 (2010).
[25] A. J. Cohen, P. Mori-Sánchez, and W. Yang, "Development of exchange-correlation functionals with minimal many-electron self-interaction error," J. Chem. Phys. **126**, 191109 (2007).
[26] V. Vlček, H. R. Eisenberg, G. Steinle-Neumann, L. Kronik, and R. Baer, "Deviations from piecewise linearity in the solid-state limit with approximate density functionals," J. Chem. Phys. **142**, 034107 (2015).
[27] D. Zhang, X. Yang, X. Zheng, and W. Yang, "Accurate density functional prediction of molecular electron affinity with the scaling corrected Kohn–Sham frontier orbital energies," Mol. Phys. **116**, 927–934 (2018).
[28] A. Görling, "Exchange-correlation potentials with proper discontinuities for physically meaningful Kohn-Sham eigenvalues and band structures," Phys. Rev. B **91**, 245120 (2015).

Published under an exclusive license by AIP Publishing

[29]J. Carmona-Espíndola, J. L. Gázquez, A. Vela, and S. B. Trickey, "Generalized gradient approximation exchange energy functional with near-best semilocal performance," J. Chem. Theory Comput. **15**, 303–310 (2019).
[30]J. Carmona-Espíndola, J. L. Gázquez, A. Vela, and S. B. Trickey, "Negative electron affinities and derivative discontinuity contribution from a generalized gradient approximation exchange functional," J. Phys. Chem. A **124**, 1334–1342 (2020).
[31]J. P. Perdew and M. Levy, "Physical content of the exact Kohn-Sham orbital energies: Band gaps and derivative discontinuities," Phys. Rev. Lett. **51**, 1884–1887 (1983).
[32]L. J. Sham and M. Schlüter, "Density functional theory of the energy gap," Phys. Rev. Lett. **51**, 1888–1891 (1983).
[33]W. Kohn, "Discontinuity of the exchange-correlation potential from a density-functional viewpoint," Phys. Rev. B **33**, 4331–4333 (1986).
[34]J. P. Perdew and M. Levy, "Comment on 'significance of the highest occupied Kohn-Sham eigenvalue,'" Phys. Rev. B **56**, 16021–16028 (1997).
[35]E. Sagvolden and J. P. Perdew, "Discontinuity of the exchange-correlation potential: Support for assumptions used to find it," Phys. Rev. A **77**, 012517 (2008).
[36]M. Hoffmann-Ostenhof and T. Hoffmann-Ostenhof, "'Schrödinger inequalities' and asymptotic behavior of electron density of atoms and molecules," Phys. Rev. A **16**, 1782–1785 (1977).
[37]Y. Tal, "Asymptotic behavior of ground state charge density in atoms," Phys. Rev. A **18**, 1781–1783 (1978).
[38]M. Levy, J. P. Perdew, and V. Sahni, "Exact differential equation for the density and ionization energy of a many-particle system," Phys. Rev. A **30**, 2745–2748 (1984).
[39]R. Armiento and S. Kümmel, "Orbital localization, charge transfer, and band gaps in semilocal density-functional theory," Phys. Rev. Lett. **111**, 036402 (2013).
[40]J. P. Perdew, K. Burke, and M. Ernzerhof, "Generalized gradient approximation made simple," Phys. Rev. Lett. **77**, 3865–3868 (1996); Erratum **78**, 1396 (1997).
[41]J. P. Perdew, "Density-functional approximation for the correlation-energy of the inhomogeneous electron-gas," Phys. Rev. B **33**, 8822–8824 (1986).
[42]J. Sun, A. Ruzsinszky, and J. P. Perdew, "Strongly constrained and appropriately normed semilocal density functional," Phys. Rev. Lett. **115**, 036402 (2015).
[43]C. Adamo and V. Barone, "Toward reliable density functional methods without adjustable parameters: The PBE0 model," J. Chem. Phys. **110**, 6158–6170 (1999).
[44]M. Ernzerhof and G. E. Scuseria, "Assessment of the Perdew–Burke–Ernzerhof exchange-correlation functional," J. Chem. Phys. **110**, 5029–5036 (1999).
[45]J. Heyd, G. E. Scuseria, and M. Ernzerhof, "Hybrid functionals based on a screened Coulomb potential," J. Chem. Phys. **118**, 8207–8215 (2003).
[46]A. V. Krukau, O. A. Vydrov, A. F. Izmaylov, and G. E. Scuseria, "Influence of the exchange screening parameter on the performance of screened hybrid functionals," J. Chem. Phys. **125**, 224106 (2006).
[47]A. D. Becke, "Density-functional thermochemistry. III. The role of exact exchange," J. Chem. Phys. **98**, 5648–5652 (1993).
[48]C. Lee, W. Yang, and R. G. Parr, "Development of the Colle-Salvetti correlation-energy formula into a functional of the electron-density," Phys. Rev. B **37**, 785–789 (1988).
[49]P. J. Stephens, F. J. Devlin, C. F. Chabalowski, and M. J. Frisch, "*Ab initio* calculation of vibrational absorption and circular-dichroism spectra using density-functional force-fields," J. Phys. Chem. **98**, 11623–11627 (1994).
[50]W. J. Hehre, R. Ditchfield, and J. A. Pople, "Self-consistent molecular orbital methods. XII. Further extensions of Gaussian-type basis sets for use in molecular-orbital studies of organic molecules," J. Chem. Phys. **56**, 2257–2261 (1972).
[51]P. C. Hariharan and J. A. Pople, "Influence of polarization functions on molecular-orbital hydrogenation energies," Theor. Chim. Acta **28**, 213–222 (1973).
[52]R. G. Parr, L. von Szentpály, and S. Liu, "Electrophilicity index," J. Am. Chem. Soc. **121**, 1922–1924 (1999).
[53]L. A. Curtiss, P. C. Redfern, K. Raghavachari, and J. A. Pople, "Gaussian-3X (G3X) theory: Use of improved geometries, zero-point energies, and Hartree–Fock basis sets," J. Chem. Phys. **114**, 108–117 (2001).
[54]W. J. Hehre, L. Radom, P. von Ragué Schleyer, and J. A. Pople, *Ab Initio Molecular Orbital Theory* (Wiley, New York, 1986).
[55]R. A. Kendall, T. H. Dunning, and R. J. Harrison, "Electron affinities of the first-row atoms revisited. Systematic basis sets and wave-functions," J. Chem. Phys. **96**, 6796–6806 (1992).
[56]D. E. Woon and T. H. Dunning, "Gaussian-basis sets for use in correlated molecular calculations. III. The atoms aluminum through argon," J. Chem. Phys. **98**, 1358–1371 (1993).
[57]M. Valiev, E. J. Bylaska, N. Govind, K. Kowalski, T. P. Straatsma, H. J. J. Van Dam, D. Wang, J. Nieplocha, E. Apra, T. L. Windus, and W. A. de Jong, "NWChem: A comprehensive and scalable open-source solution for large scale molecular simulations," Comput. Phys. Commun. **181**, 1477–1489 (2010).
[58]G. Kresse and J. Hafner, "*Ab initio* molecular dynamics for liquid metals," Phys. Rev. B **47**, 558–561 (1993).
[59]G. Kresse and J. Hafner, "*Ab initio* molecular-dynamics simulation of the liquid-metal–amorphous-semiconductor transition in germanium," Phys. Rev. B **49**, 14251–14269 (1994).
[60]G. Kresse and J. Furthmüller, "Efficiency of ab-initio total energy calculations for metals and semiconductors using a plane-wave basis set," Comput. Mater. Sci. **6**, 15–50 (1996).
[61]G. Kresse and J. Furthmüller, "Efficient iterative schemes for *ab initio* total-energy calculations using a plane-wave basis set," Phys. Rev. B **54**, 11169–11186 (1996).
[62]G. Kresse and D. Joubert, "From ultrasoft pseudopotentials to the projector augmented-wave method," Phys. Rev. B **59**, 1758–1775 (1999).
[63]P. Borlido, T. Aull, A. W. Huran, F. Tran, M. A. L. Marques, and S. Botti, "Large-scale benchmark of exchange-correlation functionals for the determination of electronic band gaps of solids," J. Chem. Theory Comput. **15**, 5069–5079 (2019).
[64]B. Patra, S. Jana, L. A. Constantin, and P. Samal, "Efficient band gap prediction of semiconductors and insulators from a semilocal exchange-correlation functional," Phys. Rev. B **100**, 045147 (2019).
[65]D. Mejia-Rodriguez and S. B. Trickey, "Deorbitalized meta-GGA exchange-correlation functionals in solids," Phys. Rev. B **98**, 115161 (2018).
[66]Z.-H. Yang, H. Peng, J. Sun, and J. P. Perdew, "More realistic band gaps from meta-generalized gradient approximations: Only in a generalized Kohn-Sham scheme," Phys. Rev. B **93**, 205205 (2016).

Published under an exclusive license by AIP Publishing